Isoform- and cell cycle–dependent substrate degradation by the Fbw7 ubiquitin ligase

Jonathan E. Grim,[1,2] Michael P. Gustafson,[1,3] Roli K. Hirata,[4] Amanda C. Hagar,[1,2] Jherek Swanger,[1,2] Markus Welcker,[1,2] Harry C. Hwang,[1,2] Johan Ericsson,[5] David W. Russell,[4] and Bruce E. Clurman[1,2]

[1]Divisions of Clinical Research and [2]Human Biology, Fred Hutchinson Cancer Research Center, Seattle, WA 98109
[3]Mayo Clinic, Rochester, MN 55905
[4]Division of Hematology, University of Washington School of Medicine, Seattle, WA 98109
[5]Ludwig Institute for Cancer Research, 751 24 Uppsala, Sweden

The SCF^{FBW7} ubiquitin ligase degrades proteins involved in cell division, growth, and differentiation and is commonly mutated in cancers. The Fbw7 locus encodes three protein isoforms that occupy distinct subcellular localizations, suggesting that each has unique functions. We used gene targeting to create isoform-specific Fbw7-null mutations in human cells and found that the nucleoplasmic Fbw7α isoform accounts for almost all Fbw7 activity toward cyclin E, c-Myc, and sterol regulatory element binding protein 1. Cyclin E sensitivity to Fbw7 varies during the cell cycle, and this correlates with changes in cyclin E–cyclin-dependent kinase 2 (CDK2)–specific activity, cyclin E autophosphorylation, and CDK2 inhibitory phosphorylation. These data suggest that oscillations in cyclin E–CDK2-specific activity during the cell cycle regulate the timing of cyclin E degradation. Moreover, they highlight the utility of adeno-associated virus–mediated gene targeting in functional analyses of complex loci.

Introduction

SCFs are multisubunit ubiquitin ligases that catalyze protein degradation by bringing substrates into proximity with ubiquitin-conjugating enzymes (Deshaies, 1999; Willems et al., 2004). F-box proteins are the SCF components that bind to substrates, and this often requires substrate phosphorylation within motifs termed phosphodegrons. Fbw7 (also called hCdc4 or hSel10) is a member of a family of F-box proteins that bind to substrates via WD40 repeats (Welcker and Clurman, 2008). The consensus motif recognized by Fbw7 was first determined for its yeast orthologue, Cdc4, and is called a Cdc4 phosphodegron (CPD; Nash et al., 2001).

Fbw7 degrades proteins with key roles in cell division, growth, and differentiation, including cyclin E, c-Myc, Notch, c-Jun, sterol regulatory element binding proteins (SREBPs), and PGC-1α (Gupta-Rossi et al., 2001; Koepp et al., 2001; Moberg et al., 2001; Oberg et al., 2001; Strohmaier et al., 2001; Nateri et al., 2004; Welcker et al., 2004b; Yada et al., 2004; Sundqvist et al., 2005; Wei et al., 2005; O'Neil et al., 2007; Thompson et al., 2007; Olson et al., 2008). Cyclin E is the most thoroughly studied substrate and contains two CPDs that are phosphorylated by glycogen synthase kinase 3β and autophosphorylated by CDK2 (Koepp et al., 2001; Strohmaier et al., 2001; Welcker et al., 2003; Ye et al., 2004).

Many Fbw7 substrates are protooncogenes that are activated when Fbw7 is disabled, and Fbw7 is an important tumor suppressor (Akhoondi et al., 2007; Welcker and Clurman, 2008). Constitutive Fbw7 disruption in mice causes embryonic lethality, whereas conditional Fbw7 ablation in T cells induces lymphomas (Tetzlaff et al., 2004; Tsunematsu et al., 2004; Onoyama et al., 2007). Fbw7 inactivation by homologous recombination in human Hct116 colon carcinoma cells causes genetic instability associated with cyclin E activation (Rajagopalan et al., 2004).

The Fbw7 gene encodes three protein isoforms (Fbw7α, Fbw7β, and Fbw7γ) generated by alternative splicing of unique 5′ exons to 10 shared exons. Each isoform is expressed from a distinct promoter, thereby allowing differential isoform expression. Importantly, the 5′ exons contain signals that direct the isoforms to distinct subcellular compartments (Fbw7α is nucleoplasmic, Fbw7β is cytoplasmic, and Fbw7γ is nucleolar; Welcker et al., 2004a). Although a few isoform-specific functions have been described (e.g., nucleolar regulation of c-Myc by Fbw7γ and recruitment of Pin1 to cyclin E by Fbw7α; Welcker et al., 2004a; van Drogen et al., 2006), these studies

Correspondence to Bruce E. Clurman: bclurman@fhcrc.org

Abbreviations used in this paper: AAV, adeno-associated virus; CPD, Cdc4 phosphodegron; P382, proline 382; SREBP, sterol regulatory element binding protein; Y15, tyrosine 15.

The online version of this paper contains supplemental material.

The Rockefeller University Press $30.00
J. Cell Biol. Vol. 181 No. 6 913–920
www.jcb.org/cgi/doi/10.1083/jcb.200802076

have used overexpression approaches. In fact, little is known about the roles of the endogenous Fbw7 isoforms in regulating substrates. To clarify these issues, we used a gene-targeting approach using adeno-associated virus (AAV) vectors to create a series of homozygous isoform-specific Fbw7-null mutations in human colon carcinoma cells.

Results and discussion

Fbw7α is the most highly expressed and stable Fbw7 isoform

We used isoform-specific real-time PCR to quantitate endogenous Fbw7 mRNA in exponentially growing human cells. We examined two transformed cell lines (Hct116 and U2OS) and two primary cell types (foreskin fibroblasts and CD34+ umbilical cord blood cells). In each case, Fbw7α was most highly expressed, and was between 8- and 50-fold more abundant than Fbw7β and 67- and 135-fold more abundant than Fbw7γ (Fig. 1 A). Transfection of equal amounts of Fbw7 expression plasmids results in much higher amounts of Fbw7α than either Fbw7β or Fbw7γ (unpublished data). We thus examined the stability of ectopic FLAG-Fbw7 proteins because we can only detect the endogenous Fbw7α protein (Fig. 1 D). Fbw7α was stable ($t_{1/2} > 6$ h), whereas the other two isoforms were labile ($t_{1/2} < 1$ h; Fig. 1 B). The high amount of Fbw7α mRNA expression and its prolonged protein stability suggested that it is the most abundant protein isoform, and this was confirmed in Western analyses of endogenous protein (Fig. 1 D). However, because the three isoforms reside in distinct subcellular locations, their relative concentrations within these compartments are unknown.

A gene-targeting strategy to create isoform-specific Fbw7 knockouts

We used AAV gene-targeting vectors to homozygously disrupt each Fbw7 isoform in Hct116 cells (Hirata et al., 2002). The targeting vectors inactivated the isoform-specific exons by the insertion of a selectable marker flanked by LoxP sites. After Cre-mediated excision of the selectable marker, stop codons were left behind in all three reading frames (Fig. 1 C). We also made a vector that simultaneously disrupts all three Fbw7 isoforms by targeting exon 2 (termed Fbw7-null hereafter). The targeting efficiency of the various vectors ranged from 0.5 to 10% of the neomycin-resistant clones analyzed (unpublished data). Homozygous-null cells were obtained by two successive rounds of targeting. Cre-adenovirus was used to remove the neo cassette after each recombination. Correctly targeted and recombined clones were confirmed by PCR, Southern blotting, and genomic sequencing (not depicted and Fig. S1, available at http://www.jcb.org/cgi/content/full/jcb.200802076/DC1). Multiple independent clones were obtained with each construct to eliminate phenotypes caused by clonal variation.

Fig. 1 D shows that Fbw7α protein is readily detected in the wild-type, Fbw7β-, and Fbw7γ-null cell lines but is absent from either Fbw7α-null or the Fbw7-null cells, confirming that

A

Fbw7 mRNA (10^{-15} moles/μg total RNA)

Cell Type	Alpha	Beta	Gamma
U2OS	7.88± 0.11	0.74± 0.21	0.058± 0.015
HCT116	5.00± 0.17	0.10± 0.01	0.050± 0.001
HFF	5.24± 0.31	0.15± 0.01	0.057± 0.004
HCB	4.44± 0.23	0.54± 0.29	0.066± 0.007

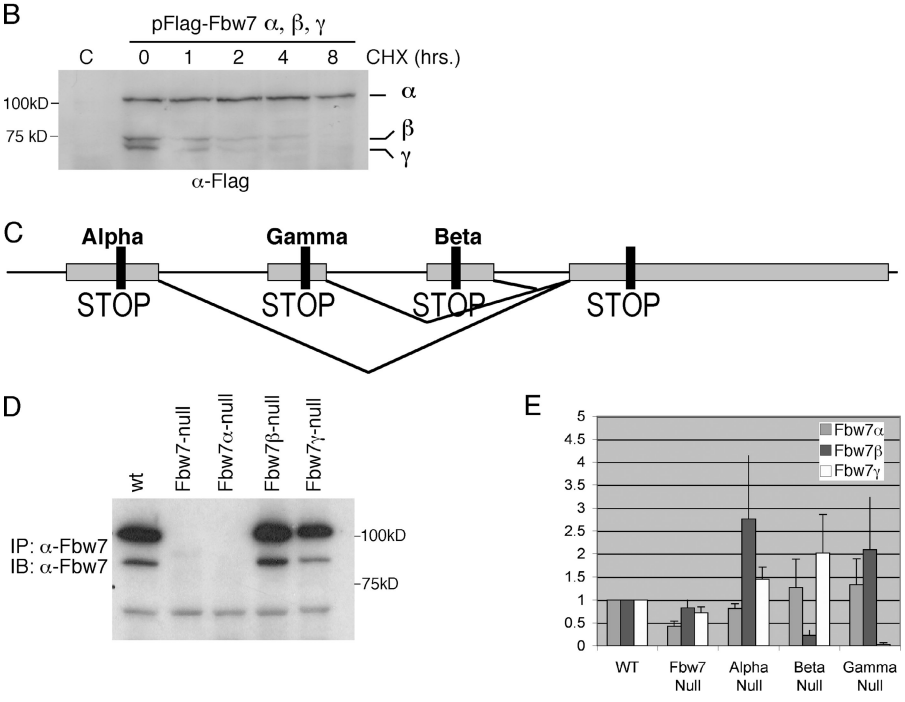

Figure 1. **Expression and targeted inactivation of Fbw7 isoforms.** (A) Fbw7 isoform mRNA abundance in the indicated cell types. (B) 293A cells were cotransfected with vectors encoding FLAG-tagged Fbw7 (0.3 μg Fbw7α and 3 μg each of Fbw7β and Fbw7γ) and treated with cycloheximide (CHX) as indicated. The three isoforms are indicated. (C) Schematic demonstrating locations of inserted stop codons for each knockout genotype (see text). (D) Lysates were prepared from confluent p150 plates of Hct116 clones of the indicated genotypes and immunoprecipitated with polyclonal anti-Fbw7 antibody followed by immunoblotting with monoclonal anti-Fbw7 antibody. (E) Real-time PCR analysis of relative Fbw7 isoform mRNA expression in Hct116 Fbw7 knockout cells. Results are expressed as relative to wild-type Hct116 cells. Error bars show standard deviation (three replicates).

the knockout strategy produced null mutations. We could not detect endogenous Fbw7β or Fbw7γ protein. We used real-time PCR assays to quantitate the Fbw7 isoform mRNAs in each Fbw7 knockout genotype (Fig. 1 E). Each of the isoform-specific targeted insertions led to reduced levels of their cognate mRNAs (but not the nontargeted isoform mRNAs), and this likely resulted from nonsense-mediated decay. This was most apparent with Fbw7γ (96% mRNA reduction) and Fbw7β (80% mRNA reduction). Inactivation of either Fbw7α or Fbw7γ modestly increased Fbw7β mRNA expression. As Fbw7β is a known target of p53 (Kimura et al., 2003), this may be because of the fact that p53 activity is mildly induced by Fbw7-loss (unpublished data). No similar compensatory increases in the expression of either Fbw7α or Fbw7γ were seen in any of the genotypes.

Isoform-specific regulation of Fbw7 substrates

We examined cyclin E, c-Myc, SREBP1, c-Jun, and Notch in the Fbw7 knockout cell series. Although c-Myc abundance was similar in all five genotypes, its turnover was greatly prolonged in the Fbw7-null and Fbw7α-null cells (Fig. 2, A and B). We previously found that Fbw7γ regulated the nucleolar pool of c-Myc in U2OS cells (Welcker et al., 2004a); however, we could not detect nucleolar c-Myc staining in any of the Hct116 cell lines (unpublished data), possibly reflecting cell type–specific differences. We used real-time PCR to address the paradox that Fbw7α-loss delayed c-Myc turnover but did not elevate its steady-state abundance (Fig. 2 C). We found that c-myc mRNA was reduced by ∼60% in Fbw7-null and Fbw7α-null cells but less so in the other cell lines. These findings are consistent with autoregulation, whereby c-Myc protein overexpression represses c-myc transcription (Grandori et al., 2000), but other homeostatic mechanisms may also attenuate changes in c-Myc steady-state abundance after Fbw7 inactivation.

The Fbw7-null and Fbw7α-null cells contained high levels of SREBP relative to the other knockout genotypes (Fig. 2 D, left). This was most apparent when we used a pT426-phosphospecific antibody, which recognizes a phosphorylated and active form of SREBP1 (Fig. 2 D, right; Sundqvist et al., 2005). Thus Fbw7α accounts for the majority of Fbw7 activity toward both c-Myc and SREBP1 in Hct116 cells. We note, however, that like cyclin E, these proteins are predominantly nucleoplasmic. We also examined c-Jun and Notch in the knockout cell lines. We did not find any consequences of Fbw7 deletion in c-Jun turnover in several contexts in the Hct116 series (unpublished data), possibly reflecting redundant turnover pathways. Moreover, Notch activity was barely detectable in Hct116 cells, and we could not perform further analyses of this pathway.

Isoform-specific cyclin E regulation

Fbw7 specifically degrades cyclin E that is autophosphorylated and catalytically active, and assays that detect cyclin E–associated kinase activity or cyclin E CPD phosphorylations (pT62, pT380, and pS384) are sensitive measures of cyclin E degradation by Fbw7. Cyclin E abundance and kinase activity were elevated in exponentially growing Fbw7-null and Fbw7α-null cells but normal in Fbw7β-null and Fbw7γ-null cells (Fig. 3 A). Because Fbw7

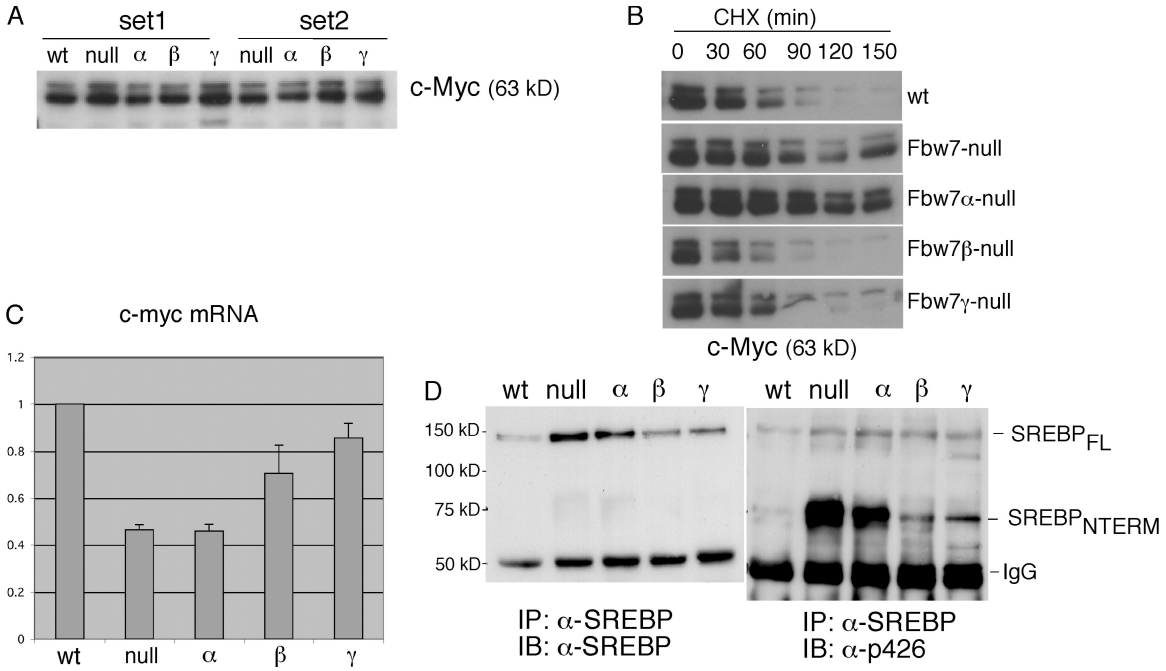

Figure 2. **c-Myc and SREBP1 regulation in Fbw7-null cells.** (A) Lysates from two independent sets of targeted Hct116 cells were immunoblotted for c-Myc or Grb2 (see Fig. 3 A for Grb2 panel). (B) Fbw7 knockout Hct116 cells were treated with cycloheximide as indicated, and lysates were immunoblotted for c-Myc. (C) Real-time PCR analysis of c-Myc mRNA in the indicated Hct116 cells. Results are expressed as relative to wild-type Hct116 cells. Error bars show standard deviation (three replicates). (D) Lysates from the indicated Hct116 cells were immunoprecipitated with anti-SREBP1 antibody and immunoblotted for either total SREBP1 (left) or pT426 SREBP1 (right).

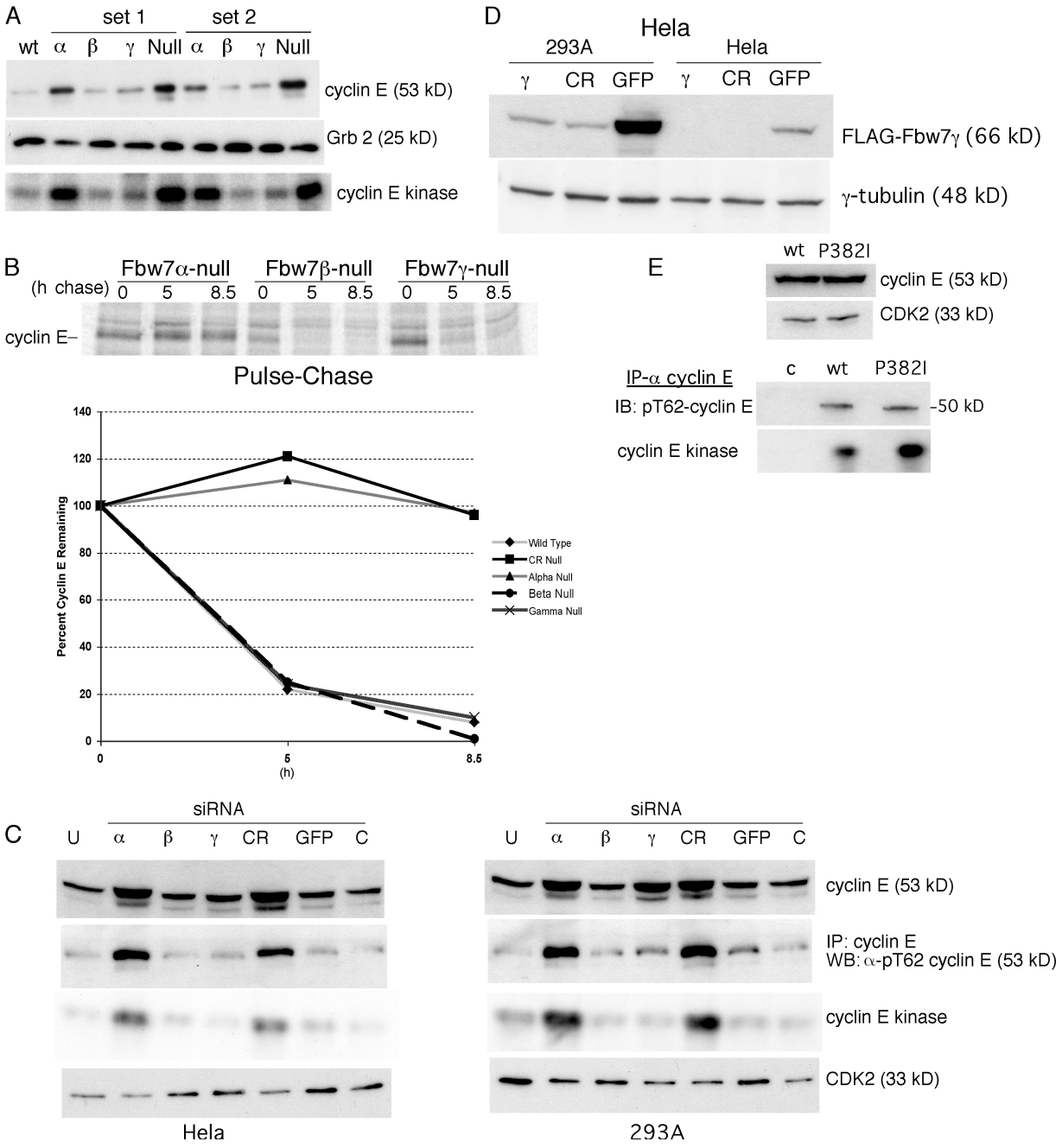

Figure 3. **Isoform-specific cyclin E regulation by Fbw7.** (A) Lysates from two independent clones of each Hct116 genotype were analyzed for cyclin E abundance and kinase activity (Grb2, loading control). (B) Pulse-chase analysis of cyclin E in Hct116 knockout lines. Cells were labeled 1 h after release from aphidicolin arrest (see text). Quantitation of the phosphorimage is depicted in the graph, and the primary data for each isoform-specific cell line is shown. (C) HeLa cells and 293A cells were transfected with the indicated Fbw7 siRNAs (α, β, γ, and CR) or control siRNAs (GFP and C). Cyclin E abundance, kinase activity, and T62 phosphorylation were measured 72 h after transfection. (D) 293A cells and HeLa cells were cotransfected with a FLAG-Fbw7γ expression vector in combination with the indicated siRNAs (γ-tubulin, loading control). (E) 293A cells were transfected with vectors expressing myc-tagged wild-type or P382I cyclin E. Lysates were immunoprecipitated with anti-Myc tag antibody (9E10), and cyclin E abundance, kinase activity, and T62 phosphorylation are shown.

deletions in mice reduce cyclin E mRNA expression (Tetzlaff et al., 2004; Tsunematsu et al., 2004), we examined cyclin E mRNA in all five genotypes and did not observe any significant differences between the cell lines (Fig. S2, available at http://www.jcb.org/cgi/content/full/jcb.200802076/DC1). We also measured cyclin E degradation rates in each Fbw7 knockout line by labeling cells after synchronization in S-phase and found that cyclin E half-life was greatly prolonged in the Fbw7-and Fbw7α-null cells but normal in the Fbw7β- and Fbw7γ-null cells (Fig. 3 B). Thus, Fbw7α accounts for most cyclin E degradation by the Fbw7 pathway. We note, however, that complete Fbw7 loss leads to somewhat higher steady-state cyclin E abundance than Fbw7α loss (Fig. 3 A), but the basis of this difference remains unclear.

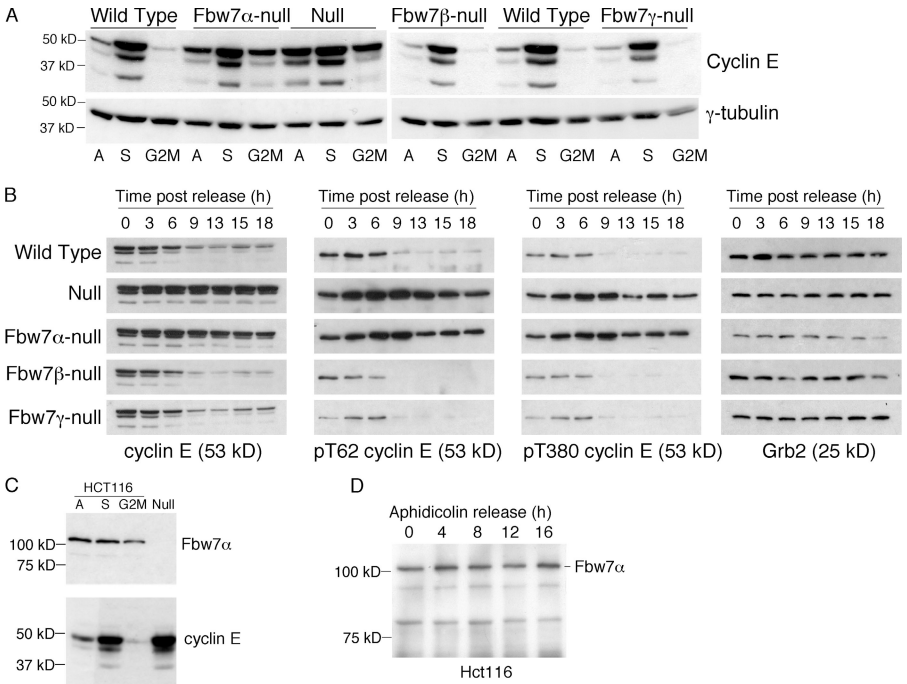

Figure 4. **Cyclin E sensitivity to Fbw7 varies during the cell cycle.** (A) The indicated Hct116 cells were treated with either aphidicolin (S), nocodazole (G2M), or DMSO (A) for 16 h, and lysates were analyzed by Western blot (γ-tubulin, loading control). Cyclin E abundance is shown. In each case, >90% of the nocodazole-arrested cells were in G2M and >70% of the aphidicolin-arrested cells were in S phase (not depicted). (B) The indicated Hct116 cell clones were arrested in S phase with a sequential thymidine/hydroxyurea block and released for the indicated time periods. The abundance of cyclin E, phosphorylated cyclin E species, and Grb2 (loading control) are shown. (C) Hct116 cells were treated as in A and lysates were examined for Fbw7 and cyclin E expression. Fbw7-null cell lysates serve as negative control. (D) Hct116 cells were arrested and released from aphidicolin and Fbw7 abundance was determined.

Our findings indicate that Fbw7α is largely responsible for cyclin E regulation in Hct116 cells, whereas the other isoforms are dispensable. However, a recent study found that both Fbw7α and Fbw7γ are sequentially required for cyclin E degradation in 293A cells (van Drogen et al., 2006). In this work, Fbw7α did not directly ubiquitinylate cyclin E but instead promoted cyclin E proline 382 (P382) isomerization by Pin1, after which cyclin E was ubiquitinylated by Fbw7γ. To address this discrepancy, we used siRNA to inhibit each Fbw7 isoform or all three isoforms together in two cell lines. We confirmed the findings of van Drogen et al. (2006) in that Fbw7γ knockdown increased cyclin E abundance in 293A cells (Fig. 3 C, right). In contrast, Fbw7γ knockdown did not alter cyclin E abundance in HeLa cells (Fig. 3 C, left). Fbw7γ knockdown was verified by using a FLAG-Fbw7γ reporter (Fig. 3 D).

Surprisingly, unlike the Fbw7α or common region siRNAs, Fbw7γ knockdown in 293A cells did not increase cyclin E kinase activity or cyclin E–phosphorylated species (Fig. 3 C). Because Fbw7γ was found to target cyclin E for degradation after cyclin E P382 isomerization, we considered the possibility that P382 isomerization inactivates cyclin E and that the cyclin E–CDK2 that accumulates after Fbw7γ knockdown in 293A cells is P382 isomerized, catalytically inactive, and stable. We thus tested a cyclin E P382I mutant that was found to be degraded by Fbw7γ alone and presumably mimics P382 isomerization. This mutant was active and phosphorylated in 293A cells, suggesting that P382 isomerization does not inactivate cyclin E–CDK2. Overall, our studies show that Fbw7γ is not required for cyclin E degradation in the cell types and assays we have examined. However, both Fbw7α and Fbw7γ may regulate cyclin E degradation in other contexts (van Drogen et al., 2006; Sangfelt et al., 2008) and more work is needed to fully understand the complex relationships between cyclin E and Fbw7.

Cell cycle–dependent cyclin E regulation

Because cyclin E degradation is triggered by autophosphorylation, we had predicted that it would be most severely affected by Fbw7 loss in S phase, when cyclin E–CDK2 activity normally peaks. We thus compared cyclin E abundance in asynchronous cells, early S-phase cells, and prometaphase cells (Fig. 4 A). Surprisingly, cyclin E abundance in S-phase cells was similar among all five Fbw7 genotypes, and the major difference attributable to Fbw7 deletion was found in prometaphase cells. Deletion of either Fbw7β or Fbw7γ did not significantly alter cyclin E abundance in any cell cycle phase.

We next released S-phase–synchronized cells from arrest and found that cyclin E abundance rapidly declined in the parental Hct116 cells but was maintained at high levels in Fbw7-null and Fbw7α-null cells (Fig. 4 B). This was most apparent when we examined the amount of T62- and T380-phosphorylated cyclin E, which are the central phosphorylation sites in the two cyclin E CPDs and specifically accumulate when Fbw7 is inactivated. Cyclin E phosphorylated on T62 and T380 abruptly declined between 6 to 9 h after release in wild-type cells but remained stable in Fbw7-null and Fbw7α-null cells. Cell cycle kinetics was similar in all five genotypes (unpublished data).

The relative sensitivity of cyclin E to Fbw7 in different cell cycle phases could result from changes in either Fbw7 or cyclin E. However, Fbw7 protein expression did not vary when cells were arrested in aphidicolin or nocodazole (Fig. 4 C) or after release from an S-phase arrest (Fig. 4 D). Thus, changes in Fbw7 abundance are unlikely to account for cell cycle–specific cyclin E degradation.

Because the synchronization experiments in Fig. 4 (A–D) used pharmacologic S-phase inhibitors that can trigger checkpoint responses that inhibit cyclin E–CDK2 autophosphorylation, we used siRNA to knockdown Fbw7 in HeLa cells (which are readily and synchronously released from nocodazole) and

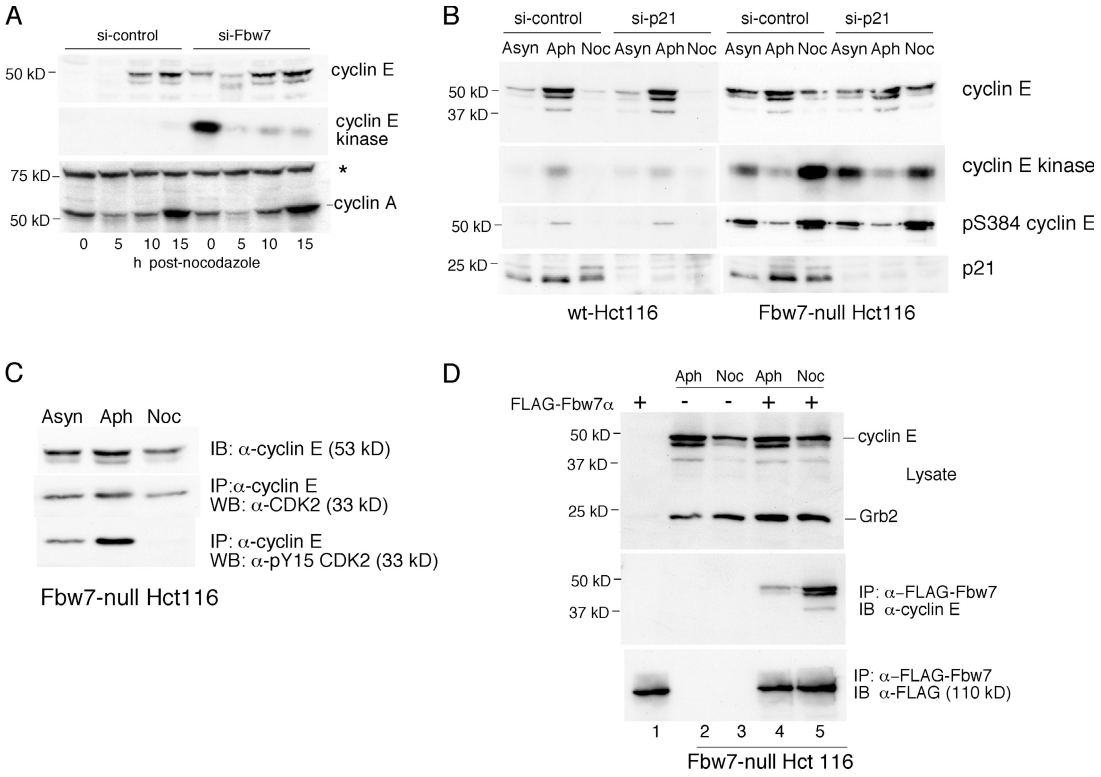

Figure 5. **Cyclin E–CDK2 activity varies during the cell cycle.** (A) HeLa cells were transfected with either control or Fbw7-siRNA and then 48 h later were treated with nocodazole for 16 h. Mitotic cells were shaken off and replated for the indicated times. Cyclin E abundance and activity, as well as cyclin A abundance (a marker of cell cycle synchronization) are shown (*, background band). (B) Hct116 cells or Fbw7-null Hct116 cells were transfected with either control or p21Cip1-specific siRNAs and, after 48 h, treated with aphidicolin (Aph) or nocodazole (Noc). Cyclin E abundance, activity, and S384 phosphorylation are shown. The efficacy of p21 knockdown is shown. (C) Fbw7-null Hct116 cells were treated with aphidicolin or nocodazole and lysates were immunoprecipitated with anti–cyclin E antibody. The amount of CDK2 and Y15–phosphorylated CDK2 bound to cyclin E is shown. (D) Increased Fbw7 binding of cyclin E obtained from mitotic Fbw7-null lysates. Compare the amount of cyclin E that coprecipitates with Fbw7 in lanes 4 and 5 (middle).

examined cyclin E as cells traversed through G1 and S phase without using S-phase inhibitors (Fig. 5 A). Again, we found that the consequences of Fbw7 inactivation were minimal in S-phase cells (10–15 h after release) compared with prometaphase cells (0 time point). The cell cycle kinetics in wild-type and Fbw7-null cells were similar, as demonstrated by the timing of cyclin A expression (Fig. 5 A) and flow cytometry (not depicted).

One striking observation in HeLa cells treated with Fbw7 siRNA (and Fbw7-null Hct116 cells; Fig. 5 B) was the very high specific activity of cyclin E–CDK2 in prometaphase cells compared with S-phase cells. That is, although S-phase cells contain more cyclin E protein than nocodazole-arrested cells, the cyclin E–CDK2 immunoprecipitated from prometaphase cells is much more active. Because cyclin E degradation is triggered by autophosphorylation, these differences in specific activity could underlie the differential sensitivity of cyclin E to Fbw7 during the cell cycle.

CDK2 activity can be regulated by CDK inhibitors or by inhibitory phosphorylations on threonine 14 and tyrosine 15 (Y15). We evaluated both of these pathways in wild-type and Fbw7-null cells. p21 is a major regulator of CDK2 activity in some cell types (e.g., fibroblasts) and is degraded in prometaphase cells by the anaphase-promoting complex (Amador et al., 2007). We used siRNA to determine if p21 was preventing cyclin E degradation in S-phase cells (Fig. 5 B). In wild-type Hct116 cells, cyclin E expression, activity, and S384 phosphorylation (an autophosphorylation site that functions as a reporter of cyclin E kinase activity [Geng et al., 2007]) all peaked in S phase and were lowest in G2/M cells, and this was not affected by p21 knockdown. However, cyclin E exhibited an inverse activity pattern in Fbw7-null cells: S-phase cells contained the highest amount of cyclin E protein yet the lowest amounts of kinase activity and S384 phosphorylation. p21 knockdown did not affect either the timing or magnitude of cyclin E activation and/or phosphorylation,

We next examined the amount of pY15-CDK2 (which is inactive) that is bound to cyclin E in Fbw7-null Hct116 cells. The amount of CDK2 Y15 phosphorylation varied dramatically and was highest in S-phase cells, intermediate in asynchronous cells, and barely detectable in prometaphase cells (Fig. 5 C). Thus, the amount of CDK inhibitory phosphorylation correlated closely with cyclin E–CDK2-specific activity during the cell cycle. These findings are consistent with previous studies demonstrating loss of inhibitory CDK2 phosphorylation as cells enter mitosis (Gu et al., 1992).

These data indicate that when cyclin E–CDK2-specific activity is very high, the stoichiometry of cyclin E autophosphorylation is also high and that this likely determines the amount of cyclin E that can bind to Fbw7. To test this idea, we used transfected FLAG-tagged Fbw7α to pull down endogenous

cyclin E from Fbw7-null Hct116 cells that were synchronized in either S-phase or prometaphase (Fig. 5 D). As predicted, the amount of cyclin E that bound to Fbw7 was greatly elevated in the prometaphase cells compared with S-phase cells, even though the abundance of cyclin E protein was similar (because the cells were Fbw7 null).

In conclusion, our results show the utility of AAV-mediated gene targeting to study complex loci and reveal that a single isoform of Fbw7 is responsible for most Fbw7 functions, at least toward the substrates that we could examine. Furthermore, Fbw7-null cells provide a useful tool to clarify regulation of cyclin E during cell cycle progression. To this end, we found large variations in cyclin E–CDK2-specific activity and cyclin E autophosphorylation during the cell cycle. In S phase, cyclin E–CDK2-specific activity and the amount of cyclin E that can bind to Fbw7 is low. In contrast, prometaphase cells contain highly active cyclin E–CDK2, which leads to increased cyclin E autophosphorylation and Fbw7 binding. Thus, changes in cyclin E autophosphorylation play a critical role in regulating cyclin E periodicity during the cell cycle by determining the accessibility of cyclin E to Fbw7. Indeed, tumor cells with Fbw7 mutations exhibit loss of cyclin E periodicity (including mitotic cyclin E expression; Ekholm-Reed et al., 2004). Interestingly, cyclin E is phosphorylated on both T62 and T380 in S phase (although it is not certain that both are on the same cyclin E molecule), and our recent studies indicate that these phosphorylated forms of cyclin E can only be degraded by Fbw7 dimers (Welcker and Clurman, 2007). Thus, one possibility is that Fbw7 dimerization is limited in S phase and that this restricts cyclin E turnover. However, our data clearly show that modifications of cyclin E itself during the cell cycle regulate its interactions with Fbw7. In particular, autophosphorylation of S384 appears pivotal, as it stimulates rapid cyclin E degradation when CDK2-specific activity is high. Our data also suggest that inhibitory CDK2 phosphorylation limits S384 phosphorylation until mitosis, providing yet another level of regulation. Finally, because ectopic cyclin E activity causes genetic instability (Spruck et al., 1999; Minella et al., 2002) that may result from aberrant mitotic progression (Rajagopalan et al., 2004; Keck et al., 2007), robust cyclin E degradation in mitosis is likely to protect cells from these deleterious consequences of inappropriate cyclin E activity.

Materials and methods

Cell lines
Hct116 (J. Simon, Fred Hutchinson Cancer Research Center, Seattle, WA), human foreskin fibroblasts (W. Carter, Fred Hutchinson Cancer Research Center, Seattle, WA), 293A (S. Reed, The Scripps Research Institute, La Jolla, CA), HeLa (American Type Culture Collection), and U2OS cells (American Type Culture Collection) were maintained in DME with 10% FBS and penicillin/streptomycin.

Antibodies
Antibodies were obtained as follows: cyclin E, pT380 cyclin E, c-Myc, SREBP, cdk2, γ-tubulin, and p21 (Santa Cruz Biotechnology, Inc.); Grb2 (BD Biosciences); and anti-pY15Cdc2/CDK2 (EMD). Anti-pT62 cyclin E and -pS384 cyclin E (Geng et al., 2003; Ye et al., 2004), anti-p426 SREBP (Sundqvist et al., 2005), and monoclonal anti-Fbw7 (Nateri et al., 2004) have been previously described. Polyclonal anti-Fbw7 antisera were generated by ProSci Incorporated (Fig. S3, available at http://www.jcb.org/cgi/content/full/jcb.200802076/DC1).

Cell synchronization/flow cytometry
Cells were treated with 5 μg/ml aphidicolin (EMD), 2.5 mM thymidine (Sigma-Aldrich), 40 ng/ml nocodazole (Sigma-Aldrich), or 2 mM hydroxyurea for 16 h, and cell cycle analyses were performed using propidium iodide–based flow cytometry as previously described (Welcker et al., 2003). For release experiments, cells were washed three times with PBS and released into normal media.

Immunoprecipitations, Western blotting, kinase assays, and pulse chase
Cells were lysed in NP-40 or TENT buffer supplemented with protease and phosphatase inhibitors. Lysates were normalized and analyzed by Western blot, immunoprecipitation, or kinase assays as previously described (Clurman et al., 1996). For pulse chase, cells were treated with aphidicolin for 16 h and than washed with normal media. After 1 h, cells were starved in media without methionine, labeled for 40 min in 0.5 mCi/ml TranS^{35}-label (MP Biomedicals) and chased in normal media with 40 mg/liter methionine.

siRNA
Previously described Fbw7 isoform-specific and control siRNA oligos (van Drogen et al., 2006) were obtained from Sigma-Aldrich and siRNA targeting p21 was obtained from Cell Signaling Technology. Dharmafect was used for siRNA transfections (Thermo Fisher Scientific).

AAV targeting vector construction, viral production, and transfection
Gene targeting, including viral production, purification, and titering, vector cloning, Hct116 transfection, screening by PCR, Southern blot, and genomic sequencing, and AdCre-mediated removal of the selectable marker was performed as previously described (Russell and Hirata, 1998) or by standard techniques. Complete primer and targeting vector sequences are available upon request. A representative targeting strategy and screening are shown in Fig. S1. Adeno-Cre viral stock was a gift from J. Chamberlain (University of Washington, Seattle, WA).

Protein stability
293A cells transfected with plasmids encoding FLAG-tagged Fbw7α, Fbw7β, and Fbw7γ (Welcker et al., 2003, 2004a) were treated with 100 μg/ml cycloheximide and lysates were immunoblotted with anti-FLAG antisera (Sigma-Aldrich). For endogenous c-Myc, 200 μg/ml cycloheximide-treated cells were harvested in TENT buffer and immunoblotted with N262 antisera.

Quantitative PCR assays
Fbw7 isoform-specific primer sets included a 5′ isoform-specific primer and a shared exon 3′ primer. Total RNA was isolated from U2OS, Hct116, or human foreskin fibroblast cells using the RNeasy kit (QIAGEN). Human cord blood cell RNA was provided by I. Bernstein (Fred Hutchinson Cancer Research Center, Seattle, WA). cDNA was synthesized with the StrataScript QPCR kit (Stratagene). Quantitative PCR was performed using SYBR green quantitative PCR master mix (Invitrogen) and an ABI Prism 7700 (Applied Biosystems). Serial dilutions of plasmid DNA in total RNA were used as a standard curve for absolute quantitation of isoform mRNA levels (expressed as the molar amount of mRNA/1 μg of total RNA). Analysis of Fbw7 isoforms and of c-myc in Hct116 knockout cells used similar methods. Relative expression (normalized to RPL13) was calculated according to the manufacturer's (Applied Biosystems) instructions.

Cyclin E–FLAG–Fbw7 binding assay
Fbw7-null Hct116 cells were treated with aphidicolin or nocodazole for 16 h and lysed with TENT buffer. Equal amounts of lysate were mixed with 100 μl FLAG-Fbw7α lysate (from $CaPO_4$-transfected 293a cells) and 10 μl M2 FLAG agarose (Sigma-Aldrich), rotated for 2 h, washed, and analyzed by Western blotting.

Online supplemental material
Fig. S1 shows a general strategy for AAV gene targeting in Hct116 cells. Fig. S2 shows real-time PCR analyses of cyclin E mRNA. Fig. S3 shows production of rabbit polyclonal anti-Fbw7 antibodies. Online supplemental material is available at http://www.jcb.org/cgi/content/full/jcb.200802076/DC1.

The authors thank S. Reed for providing 293A cells and for helpful discussions.

This work was supported by grants from the National Institutes of Health (B.E. Clurman and D.W. Russell), National Institutes of Health Career Development Awards (J.E. Grim and H. Hwang), the Burroughs Welcome Foundation (B.E. Clurman), the American Society of Hematology (J.E. Grim), and the Leukemia and Lymphoma Society (M. Welcker).

Submitted: 13 February 2008
Accepted: 15 May 2008

References

Akhoondi, S., D. Sun, N. von der Lehr, S. Apostolidou, K. Klotz, A. Maljukova, D. Cepeda, H. Fiegl, D. Dofou, C. Marth, et al. 2007. FBXW7/hCDC4 is a general tumor suppressor in human cancer. *Cancer Res.* 67:9006–9012.

Amador, V., S. Ge, P.G. Santamaria, D. Guardavaccaro, and M. Pagano. 2007. APC/C(Cdc20) controls the ubiquitin-mediated degradation of p21 in prometaphase. *Mol. Cell.* 27:462–473.

Clurman, B.E., R.J. Sheaff, K. Thress, M. Groudine, and J.M. Roberts. 1996. Turnover of cyclin E by the ubiquitin-proteasome pathway is regulated by cdk2 binding and cyclin phosphorylation. *Genes Dev.* 10:1979–1990.

Deshaies, R.J. 1999. SCF and Cullin/Ring H2-based ubiquitin ligases. *Annu. Rev. Cell Dev. Biol.* 15:435–467.

Ekholm-Reed, S., C.H. Spruck, O. Sangfelt, F. van Drogen, E. Mueller-Holzner, M. Widschwendter, A. Zetterberg, and S.I. Reed. 2004. Mutation of hCDC4 leads to cell cycle deregulation of cyclin E in cancer. *Cancer Res.* 64:795–800.

Geng, Y., Q. Yu, E. Sicinska, M. Das, J.E. Schneider, S. Bhattacharya, W.M. Rideout, R.T. Bronson, H. Gardner, and P. Sicinski. 2003. Cyclin E ablation in the mouse. *Cell.* 114:431–443.

Geng, Y., Y.M. Lee, M. Welcker, J. Swanger, A. Zagozdzon, J.D. Winer, J.M. Roberts, P. Kaldis, B.E. Clurman, and P. Sicinski. 2007. Kinase-independent function of cyclin E. *Mol. Cell.* 25:127–139.

Grandori, C., S.M. Cowley, L.P. James, and R.N. Eisenman. 2000. The Myc/Max/Mad network and the transcriptional control of cell behavior. *Annu. Rev. Cell Dev. Biol.* 16:653–699.

Gu, Y., J. Rosenblatt, and D.O. Morgan. 1992. Cell cycle regulation of CDK2 activity by phosphorylation of Thr160 and Tyr15. *EMBO J.* 11:3995–4005.

Gupta-Rossi, N., O. Le Bail, H. Gonen, C. Brou, F. Logeat, E. Six, A. Ciechanover, and A. Israel. 2001. Functional interaction between SEL-10, an F-box protein, and the nuclear form of activated Notch1 receptor. *J. Biol. Chem.* 276:34371–34378.

Hirata, R., J. Chamberlain, R. Dong, and D.W. Russell. 2002. Targeted transgene insertion into human chromosomes by adeno-associated virus vectors. *Nat. Biotechnol.* 20:735–738.

Keck, J.M., M.K. Summers, D. Tedesco, S. Ekholm-Reed, L.C. Chuang, P.K. Jackson, and S.I. Reed. 2007. Cyclin E overexpression impairs progression through mitosis by inhibiting APC^{Cdh1}. *J. Cell Biol.* 178:371–385.

Kimura, T., M. Gotoh, Y. Nakamura, and H. Arakawa. 2003. hCDC4b, a regulator of cyclin E, as a direct transcriptional target of p53. *Cancer Sci.* 94:431–436.

Koepp, D.M., L.K. Schaefer, X. Ye, K. Keyomarsi, C. Chu, J.W. Harper, and S.J. Elledge. 2001. Phosphorylation-dependent ubiquitination of cyclin E by the SCFFbw7 ubiquitin ligase. *Science.* 294:173–177.

Minella, A.C., J. Swanger, E. Bryant, M. Welcker, H. Hwang, and B.E. Clurman. 2002. p53 and p21 form an inducible barrier that protects cells against cyclin E-cdk2 deregulation. *Curr. Biol.* 12:1817–1827.

Moberg, K.H., D.W. Bell, D.C. Wahrer, D.A. Haber, and I.K. Hariharan. 2001. Archipelago regulates Cyclin E levels in *Drosophila* and is mutated in human cancer cell lines. *Nature.* 413:311–316.

Nash, P., X. Tang, S. Orlicky, Q. Chen, F.B. Gertler, M.D. Mendenhall, F. Sicheri, T. Pawson, and M. Tyers. 2001. Multisite phosphorylation of a CDK inhibitor sets a threshold for the onset of DNA replication. *Nature.* 414:514–521.

Nateri, A.S., L. Riera-Sans, C. Da Costa, and A. Behrens. 2004. The ubiquitin ligase SCFFbw7 antagonizes apoptotic JNK signaling. *Science.* 303:1374–1378.

O'Neil, J., J. Grim, P. Strack, S. Rao, D. Tibbitts, C. Winter, J. Hardwick, M. Welcker, J.P. Meijerink, R. Pieters, et al. 2007. FBW7 mutations in leukemic cells mediate NOTCH pathway activation and resistance to γ-secretase inhibitors. *J. Exp. Med.* 204:1813–1824.

Oberg, C., J. Li, A. Pauley, E. Wolf, M. Gurney, and U. Lendahl. 2001. The Notch intracellular domain is ubiquitinated and negatively regulated by the mammalian Sel-10 homolog. *J. Biol. Chem.* 276:35847–35853.

Olson, B.L., M.B. Hock, S. Ekholm-Reed, J.A. Wohlschlegel, K.K. Dev, A. Kralli, and S.I. Reed. 2008. SCFCdc4 acts antagonistically to the PGC-1 {alpha} transcriptional coactivator by targeting it for ubiquitin-mediated proteolysis. *Genes Dev.* 22:252–264.

Onoyama, I., R. Tsunematsu, A. Matsumoto, T. Kimura, I.M. de Alboran, K. Nakayama, and K.I. Nakayama. 2007. Conditional inactivation of *Fbxw7* impairs cell-cycle exit during T cell differentiation and results in lymphomatogenesis. *J. Exp. Med.* 204:2875–2888.

Rajagopalan, H., P.V. Jallepalli, C. Rago, V.E. Velculescu, K.W. Kinzler, B. Vogelstein, and C. Lengauer. 2004. Inactivation of hCDC4 can cause chromosomal instability. *Nature.* 428:77–81.

Russell, D.W., and R.K. Hirata. 1998. Human gene targeting by viral vectors. *Nat. Genet.* 18:325–330.

Sangfelt, O., D. Cepeda, A. Malyukova, F. van Drogen, and S.I. Reed. 2008. Both SCF(Cdc4alpha) and SCF(Cdc4gamma) are required for cyclin E turnover in cell lines that don't overexpress cyclin E. *Cell Cycle.* 7:1077–1084.

Spruck, C.H., K.A. Won, and S.I. Reed. 1999. Deregulated cyclin E induces chromosome instability. *Nature.* 401:297–300.

Strohmaier, H., C.H. Spruck, P. Kaiser, K.A. Won, O. Sangfelt, and S.I. Reed. 2001. Human F-box protein hCdc4 targets cyclin E for proteolysis and is mutated in a breast cancer cell line. *Nature.* 413:316–322.

Sundqvist, A., M. Bengoechea-Alonso, X. Ye, V. Lukiyanchuk, J. Jin, J.W. Harper, and J. Ericsson. 2005. Control of lipid metabolism by phosphorylation-dependent degradation of the SREBP family of transcription factors by SCFFbw7. *Cell Metab.* 1:379–391.

Tetzlaff, M.T., W. Yu, M. Li, P. Zhang, M. Finegold, K. Mahon, J.W. Harper, R.J. Schwartz, and S.J. Elledge. 2004. Defective cardiovascular development and elevated cyclin E and Notch proteins in mice lacking the Fbw7 F-box protein. *Proc. Natl. Acad. Sci. USA.* 101:3338–3345.

Thompson, B.J., S. Buonamici, M.L. Sulis, T. Palomero, T. Vilimas, G. Basso, A. Ferrando, and I. Aifantis. 2007. The SCF^{FBW7} ubiquitin ligase complex as a tumor suppressor in T cell leukemia. *J. Exp. Med.* 204:1825–1835.

Tsunematsu, R., K. Nakayama, Y. Oike, M. Nishiyama, N. Ishida, S. Hatakeyama, Y. Bessho, R. Kageyama, T. Suda, and K.I. Nakayama. 2004. Mouse Fbw7/Sel-10/Cdc4 is required for notch degradation during vascular development. *J. Biol. Chem.* 279:9417–9423.

van Drogen, F., O. Sangfelt, A. Malyukova, L. Matskova, E. Yeh, A.R. Means, and S.I. Reed. 2006. Ubiquitylation of cyclin E requires the sequential function of SCF complexes containing distinct hCdc4 isoforms. *Mol. Cell.* 23:37–48.

Wei, W., J. Jin, S. Schlisio, J.W. Harper, and W.G. Kaelin Jr. 2005. The v-Jun point mutation allows c-Jun to escape GSK3-dependent recognition and destruction by the Fbw7 ubiquitin ligase. *Cancer Cell.* 8:25–33.

Welcker, M., and B.E. Clurman. 2007. Fbw7/hCDC4 dimerization regulates its substrate interactions. *Cell Div.* 2:7.

Welcker, M., and B.E. Clurman. 2008. FBW7 ubiquitin ligase: a tumour suppressor at the crossroads of cell division, growth and differentiation. *Nat. Rev. Cancer.* 8:83–93.

Welcker, M., J. Singer, K.R. Loeb, J. Grim, A. Bloecher, M. Gurien-West, B.E. Clurman, and J.M. Roberts. 2003. Multisite phosphorylation by Cdk2 and GSK3 controls cyclin E degradation. *Mol. Cell.* 12:381–392.

Welcker, M., A. Orian, J.A. Grim, R.N. Eisenman, and B.E. Clurman. 2004a. A nucleolar isoform of the Fbw7 ubiquitin ligase regulates c-Myc and cell size. *Curr. Biol.* 14:1852–1857.

Welcker, M., A. Orian, J. Jin, J.A. Grim, J.W. Harper, R.N. Eisenman, and B.E. Clurman. 2004b. The Fbw7 tumor suppressor regulates glycogen synthase kinase 3 phosphorylation-dependent c-Myc protein degradation. *Proc. Natl. Acad. Sci. USA.* 101:9085–9090.

Willems, A.R., M. Schwab, and M. Tyers. 2004. A hitchhiker's guide to the cullin ubiquitin ligases: SCF and its kin. *Biochim. Biophys. Acta.* 1695:133–170.

Yada, M., S. Hatakeyama, T. Kamura, M. Nishiyama, R. Tsunematsu, H. Imaki, N. Ishida, F. Okumura, K. Nakayama, and K.I. Nakayama. 2004. Phosphorylation-dependent degradation of c-Myc is mediated by the F-box protein Fbw7. *EMBO J.* 23:2116–2125.

Ye, X., G. Nalepa, M. Welcker, B.M. Kessler, E. Spooner, J. Qin, S.J. Elledge, B.E. Clurman, and J.W. Harper. 2004. Recognition of phosphodegron motifs in human cyclin E by the SCF(Fbw7) ubiquitin ligase. *J. Biol. Chem.* 279:50110–50119.